Cylindrical magnets and ideal solenoids

Norman Derby[a)]
Community College of Vermont, Bennington, Vermont 05201

Stanislaw Olbert[b)]
Department of Physics, Massachusetts Institute of Technology, Cambridge, Massachusetts 02139

(Received 9 June 2009; accepted 7 October 2009)

Both wire-wound solenoids and cylindrical magnets can be approximated as ideal azimuthally symmetric solenoids. We present an exact solution for the magnetic field of an ideal solenoid in an easy to use form. The field is expressed in terms of a single function that can be rapidly computed by means of a compact efficient algorithm, which can be coded as an add-in function to a spreadsheet, making field calculations accessible to introductory students. These expressions are not only accurate but are also as fast as most approximate expressions. We demonstrate their utility by simulating the dropping of a cylindrical magnet through a nonmagnetic conducting tube and comparing the calculation with data obtained from experiments suitable for an undergraduate laboratory.
[DOI: 10.1119/1.3256157]

I. INTRODUCTION

Solenoids and cylindrical magnets are staples of introductory physics laboratory experiments and demonstrations. When it comes time to put theory to the test, simple models for these objects are needed. An idealized solenoid—a solenoid with strictly azimuthal current in a thin sheet wrapped around a right circular cylinder—can serve as a reasonable model of an actual wire-wound solenoid and can serve as an even better model of a permanent cylindrical magnet, provided that its magnetization is sufficiently uniform.

The magnetic field of an ideal solenoid of finite length can be expressed in terms of elementary functions only along its symmetry axis. At off-axis points, calculation is much more difficult and introductory level students usually have no tools for obtaining even approximate values for the field except at very large distances where the field resembles that of a point dipole.

It is well known that the field due to a circular current loop can be written in terms of elliptic integrals, and thus by treating the ideal solenoid as a stack of loops, its magnetic field can be obtained by straightforward integration. Alternatively, the field may be derived by solving a boundary-value problem with cylindrical symmetry. Either way, exact expressions for the field have been known for over a century and can be expressed using various special functions such as elliptic integrals, Heuman's lambda function, various Bessel functions, and hypergeometric functions.[1–4] Some of these expressions look quite complicated and may appear difficult to use.

There are many occasions in which calculations involving solenoid fields may arise. As a convenient tool for such situations, we present an exact solution in a form that is algebraically less complicated, does not require any previous knowledge of special functions, and comes with a numerical algorithm that is simple and efficient. The field is expressed in terms of a single function, a generalized complete elliptic integral. This function is completely defined by an integral whose form occurs naturally in problems involving cylindrical symmetry. Numerical values can be computed by means of an algorithm that can be easily coded on a programmable calculator or employed as a user-defined function or macro in a spreadsheet. In this form, the finite-length ideal solenoid model is as simple and fast to use as the point dipole model.

This paper presents these exact expressions for the magnetic field of an ideal solenoid and its self-inductance and provides a brief illustration of the effectiveness of these expressions by simulating the dropping a cylindrical magnet through a nonmagnetic conducting tube and comparing the calculations with the results of some simple experiments.

II. THE GENERALIZED COMPLETE ELLIPTIC INTEGRAL

Certain integrals occur naturally in determining fields with cylindrical symmetry. They are special cases of a function defined by a generalized complete elliptic integral,

$$C(k_c,p,c,s) = \int_0^{\pi/2} \frac{(c\cos^2\varphi + s\sin^2\varphi)d\varphi}{(\cos^2\varphi + p\sin^2\varphi)\sqrt{\cos^2\varphi + k_c^2\sin^2\varphi}}. \tag{1}$$

Appendix A describes the code for an efficient numerical algorithm for calculating values for C. The example code is presented in a version of BASIC that can be directly used as a user-defined function in a spreadsheet or converted to other programming languages. Appendix A also contains further information about C, including the relation of C to other forms of elliptic integrals and links to code.

III. MAGNETIC FIELD EXPRESSIONS

Consider a cylinder of length $2b$ and radius a wrapped by an azimuthal sheet of current I_{total}, equivalent to a tightly wound solenoid with a number of turns per unit length n carrying a current I, that is, $I_{\text{total}}=2bnI$. The magnetic moment μ of the solenoid is $\mu=2bnI\pi a^2$. It is well known that along the symmetry axis of a such a solenoid, the field takes the form

$$B_z = \frac{\mu_0 nI}{2}\left\{\frac{z+b}{\sqrt{(z+b)^2+a^2}} - \frac{z-b}{\sqrt{(z-b)^2+a^2}}\right\}, \tag{2}$$

where we have used cylindrical coordinates (ρ,φ,z), with the origin at the center of the solenoid. Equation (2) reduces to $B_z=\mu_0 nI$ for an infinite solenoid. For the general case (see

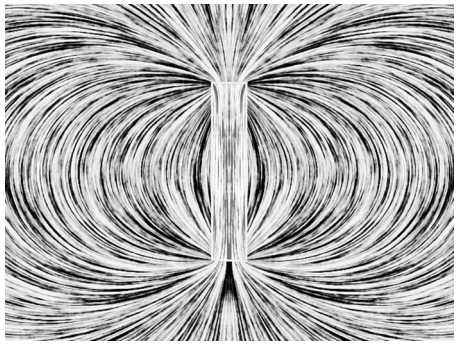

Fig. 1. Field lines of an ideal solenoid with a length that is five times its diameter.

Appendix B for an outline of the derivation), the field components are

$$B_\rho = B_0[\alpha_+ C(k_+,1,1,-1) - \alpha_- C(k_-,1,1,-1)] \tag{3}$$

and

$$B_z = \frac{B_0 a}{a+\rho}[\beta_+ C(k_+,\gamma^2,1,\gamma) - \beta_- C(k_-,\gamma^2,1,\gamma)], \tag{4}$$

with

$$B_0 = \frac{\mu_0}{\pi} nI, \tag{5}$$

$$z_\pm = z \pm b, \tag{6}$$

$$\alpha_\pm = \frac{a}{\sqrt{z_\pm^2 + (\rho+a)^2}}, \tag{7}$$

$$\beta_\pm = \frac{z_\pm}{\sqrt{z_\pm^2 + (\rho+a)^2}}, \tag{8}$$

$$\gamma = \frac{a-\rho}{a+\rho}, \tag{9}$$

$$k_\pm = \sqrt{\frac{z_\pm^2 + (a-\rho)^2}{z_\pm^2 + (a+\rho)^2}}. \tag{10}$$

These compact forms involve only the single function C. They compute quickly and accurately both inside and outside the solenoid and are mathematically well-behaved except on the edge of the current sheet at $\rho = a$ and $z = \pm b$.

Equations (3) and (4) reveal that if distances are measured in units of a, then the magnetic field lines of an ideal solenoid depend only on the ratio b/a. Figure 1 shows the field lines for a solenoid with $b = 5a$ using the line integral convolution method employed by Sundquist[5] and Belcher. Using Eqs. (3) and (4) for the field and the algorithm for C, we were able to produce the image in Fig. 1 using their program[6] in a matter of seconds. The behavior of field lines within the solenoid contrasts sharply with that of external field lines and indicates why a single approximate expression in terms of elementary functions has difficulty representing the field at both near and far distances.

A. Limits

Along the axis of the solenoid ($\rho = 0$), $k_\pm = \gamma = 1$ and $C(1,1,1,1) = \pi/2$, and thus Eq. (4) reduces to Eq. (2).

As $b \to 0$ with $2bnI = I_{\text{total}}$ remaining finite, a solenoid becomes a current loop, and the field expressions in Eqs. (3) and (4) with $0 < b \ll a$ approximate those of a current loop. For $b = 0$ they take the form

$$B_\rho = \frac{\mu_0}{\pi} \frac{I_{\text{total}} a z}{[z^2 + (\rho+a)^2]^{3/2}} C(k_1, k_1^2, -1, 1) \tag{11}$$

and

$$B_z = \frac{\mu_0}{\pi} \frac{I_{\text{total}} a(\rho+a)}{[z^2 + (\rho+a)^2]^{3/2}} C(k_1, k_1^2, 1, \gamma), \tag{12}$$

where

$$k_1^2 \equiv \frac{z^2 + (a-\rho)^2}{z^2 + (a+\rho)^2}. \tag{13}$$

At large distances from the solenoid ($r \gg a, b$), the field reduces to that of a point dipole,

$$B_\rho = \frac{\mu_0 \mu}{4\pi} \frac{3\rho z}{r^5}, \quad B_z = \frac{\mu_0 \mu}{4\pi} \frac{(2z^2 - \rho^2)}{r^5}, \tag{14}$$

with

$$r^2 = \rho^2 + z^2. \tag{15}$$

B. Inductance

It is also possible to derive an exact expression for the mutual inductance of two coaxial ideal solenoids.[7–9] The self-inductance L of a solenoid can then be obtained as a special case. In our notation the self-inductance can be expressed compactly as

$$L = \tfrac{8}{3}\mu_0 (na)^2 [\sqrt{a^2+b^2}\, C(k_0, 1, 1, 2k_0^2) - a], \tag{16}$$

where

$$k_0 = \frac{b}{\sqrt{a^2+b^2}}. \tag{17}$$

IV. FALLING MAGNETS

A. Previous work

Faraday's law is often dramatically demonstrated by dropping a small highly magnetized cylindrical permanent magnet (radius a, length $2b$, mass m, and magnetic moment μ) into a vertical nonmagnetic tube of conductivity σ, relative permeability of 1, length L, inside radius r, and wall thickness $w \ll r$ (Fig. 2).[10–15] The small masses and large magnetic moments of rare earth magnets give them a long "hang" time. After the initial surprise subsides, students begin to ask questions "How does the time of fall depend on the diameter and the conductivity of the tube?" and "How does it depend on the length of the magnet?"

This experiment or similar ones have been analyzed in several papers. Pelesko *et al.*[16] and Roy *et al.*[17] use dimensional analysis to show that in a thin-walled tube, the speed of the falling magnet is proportional to $(mgr^4)/(\sigma\mu^2 w)$, which demonstrates the power of dimensional analysis, al-

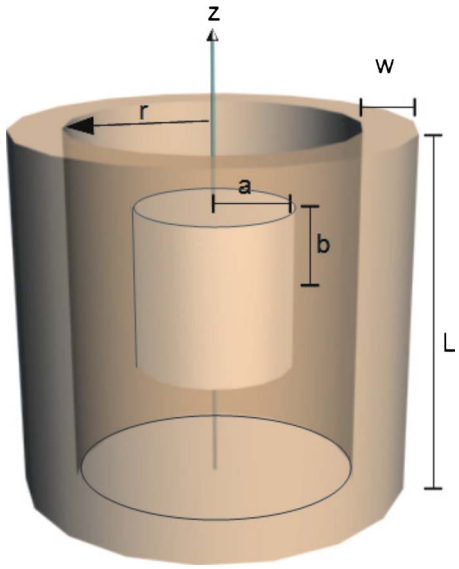

Fig. 2. Geometry for a magnet falling though a nonmagnetic conducting tube.

though it is unable to provide information about how the speed depends on the geometry of the magnet. Other papers employ Faraday's law but differ in the ways they model the cylindrical magnet. Hahn *et al.*[10] derive Eq. (27) for the force on a magnet oscillating in a tube but evaluated the force by treating the magnet as a point dipole. Knyazev *et al.*[18] treat only the point dipole case but expanded the analysis to include high speeds not attainable in demonstrations. Levin *et al.*[12] note that the ideal solenoid's external field is equivalent to that of two uniformly (magnetically) charged disks at the top and bottom of the magnet but use point monopoles instead of disks in their calculations. Iñiguez *et al.*[19] model the interaction of the magnet and the tube by means of an elaborate equivalent resistor network and provide a sample calculation in which the magnet is treated as a point dipole. Calculations based on the dipole approximation do not predict experimental results with much accuracy when the magnet fits closely within the tube, especially when the length of the magnet is greater than its diameter.

After deducing Eq. (28), MacLatchy *et al.*[20] model the cylindrical magnet as a stack of several polygonal loops and then compute its field from the Biot–Savart law. Although slightly cumbersome, this approach does offer adjustable accuracy. Partovi and Morris[21] offer a comprehensive treatment of a cylindrical magnet moving at an arbitrary nonrelativistic velocity in an infinite tube of arbitrary thickness and permeability. This is a boundary-value problem with cylindrical symmetry that they solve, expressing the drag force on the magnet in terms of integrals involving Bessel functions with complex arguments. Their results are exact, though restricted to a steady state situation. The integral expressions in their paper are daunting, but the authors provide sample *Mathematica* code for computing them.

B. Theory

Because Refs. 10, 20, and 21 discuss the theory in some detail, we provide only a quick sketch here. Choose cylindrical coordinates with the z-axis vertical and the origin located (momentarily) at the center of the magnet. The conductivity of the tube can be determined by measuring its resistance per unit length R_L,

$$R_L = \frac{1}{\sigma 2\pi w \bar{r}}, \tag{18}$$

where $\bar{r}=r+w/2$. As the magnet falls, the changing magnetic field within the tube walls is accompanied by an electric field that drives currents, which cause Ohmic heating. Although currents in the tube induce currents within the permanent magnet, it is easy to show that under our experimental conditions, the only significant energy losses are those within the tube walls. The speed of fall is so slow that air resistance is also quite negligible. In the following we assume that the magnet fits closely enough within the tube walls that its axis remains vertical and cylindrical symmetry is maintained during the fall. (When a small diameter magnet falls within a much larger diameter tube, the axis of the magnet may precess about the vertical during the fall.)

The electric field within the tube can be deduced by arguing that in the reference frame of the falling magnet, there is only a magnetostatic field. Thus in the frame of reference of the tube, where the magnet has velocity $\mathbf{v}$, there must be an electric field $\mathbf{E}=-\mathbf{v}\times\mathbf{B}$, or $E_\varphi=-v_z B_\rho$. Alternatively, the field can be obtained from Faraday's law by considering a horizontal circular loop of radius $\bar{r}$ lying within the tube walls at height z' above the center of the magnet. We define the upward magnetic flux though such a loop as

$$\Phi(z') = \int_0^{\bar{r}} B_z(\rho,z') 2\pi\rho d\rho. \tag{19}$$

The emf around the loop is

$$\text{emf} = -\frac{d\Phi}{dt} = -\frac{d\Phi(z')}{dz'}\frac{dz'}{dt} = v_z \frac{d\Phi(z)}{dz}, \tag{20}$$

where $v_z=-dz'/dt$.

If we take two such loops separated by the vertical distance dz, we can visualize them as the edges of a small cylindrical Gaussian pill box. Because there are no magnetic monopoles, the total magnetic flux leaving the closed surface of the box must be zero,

$$\Phi(z+dz) - \Phi(z) + B_\rho(\bar{r},z) 2\pi\bar{r}dz = 0 = d\Phi + B_\rho(\bar{r},z) 2\pi\bar{r}dz. \tag{21}$$

If we combine Eqs. (21) and (20), we have

$$\text{emf} = -(2\pi\bar{r}v_z)B_\rho = E_\varphi 2\pi\bar{r}. \tag{22}$$

The force acting on the falling magnet can be deduced from energy considerations. The electric field within the tube drives currents that dissipate energy at a rate per unit volume of σE_φ^2, which can be integrated over the volume of the tube's wall to obtain the total power lost P. If the walls are thin, the power loss when the magnet is at height z above the bottom of the tube is

$$P = \int \sigma E_\varphi^2 2\pi w\bar{r}dz = 2\pi w\bar{r}\sigma v_z^2 \times \int_{-z}^{L-z} B_\rho^2(\bar{r},z')dz' = -v_z F_{\text{drag}}. \tag{23}$$

Table I. Physical and electrical properties of the tube. The tube's resistance per unit length R_L was determined by connecting it to a dc power supply with alligator clips, running a current I through the length L of the tube, and measuring the potential drop ΔV from clip to clip. The electrical conductivity σ was determined using the measured values of the tube's inner radius r and wall thickness w.

Physical	Electrical
$L=1.478$ m	Length between clips $=1.475$ m
$r=7.25$ mm	$I=4.95$ A
$w=0.7$ mm	$\Delta V=4.49$ mV
Mass $=434$ g	$\sigma=56.0\times10^{6}$ S/m
	$R_L=5.37\times10^{-4}$ Ω/m

Alternatively, the Lorentz forces acting on the currents can be calculated directly. A horizontal slice of tubing of height dz located at height z above the center of the magnet is a circuit with electrical resistance

$$R_E=\frac{1}{\sigma}\frac{2\pi\bar{r}}{wdz}, \tag{24}$$

and thus the current due to the emf around the ring is

$$dI=\frac{\text{emf}}{R_E}=-\sigma v_z wB_\rho dz. \tag{25}$$

The vertical force exerted on this current by **B** is

$$dF_z=-2\pi\bar{r}dIB_\rho=\sigma 2\pi\bar{r}wv_zB_\rho^2dz, \tag{26}$$

and the force on the magnet follows from Newton's third law. The total vertical force on the magnet is the sum

$$F_{\text{drag}}=-\frac{v_z}{R_L}\int_{-z}^{L-z}B_\rho^2(\bar{r},z')dz', \tag{27}$$

in agreement with Eq. (23).

The computation of the magnetic field is so rapid using Eq. (3) for B_ρ that the drag force in Eq. (27) can be used to numerically integrate the equation of motion for the falling magnet, even though an integration must be performed at each time step.

The powerful but light-weight magnets used in demonstrations reach a constant velocity within a fraction of a second. Because the magnitude of B_ρ declines extremely rapidly with z, this terminal velocity can be calculated by equating F_{drag} to mg and, with little error, setting the limits of integration to $\pm\infty$,

$$v_{\text{terminal}}=\frac{-mgR_L}{\int_{-\infty}^{\infty}B_\rho^2(\bar{r},z')dz'}. \tag{28}$$

C. Experiment

We dropped cylindrical magnets through a long copper tube, measured the total time of fall, and then compared the results with calculations based on Eqs. (27) and (28). We used equipment available in a typical undergraduate physics laboratory and followed procedures that might be employed in an introductory level course. We used a copper plumbing tube (see Table I), which is about 99% pure copper. Its magnetic permeability was not measured but taken to be the same as pure copper. The resistance per unit length was determined by running a current of several amperes through the tube while measuring a few millivolts potential difference across it. (The conductivity of pure copper is about 110% of the standard IACS value, 5.8108×10^{7} S/m at 20 °C, and the conductivity of typical copper tubing for plumbing is typically about 85% of the IACS value.)

We obtained six cylindrical magnets with various lengths but with the same 0.5 in. (12.7 mm) diameter. We determined the magnetic moment μ for each one by using a small magnetometer to measure the field strength at several points along its axis and then adjusting the value of (nI) in Eq. (2) to give a best fit.

We held a magnet vertically by its upper 4 mm and inserted it into the top of the tube and released it while manually starting a timer that stopped when the bottom millimeter of the magnet activated a photogate placed at the bottom of the tube. The results are summarized in Table II. In addition to the measured average velocity of each falling magnet, Table II shows the terminal velocities computed from Eq. (28) and from the lengthy exact expression for the terminal velocity in Ref. 21. (Both calculations were programmed in *Python* using the *SciPy* libraries and a *Python* version of the function C.) The numerical agreement between these two ways of computing the terminal velocity validates the approximations used in deriving Eq. (28).

We also used Eq. (27) for the drag force on a falling magnet to numerically solve the equations of motion for $z(t)$ and

Table II. Properties of the six cylindrical magnets with 0.5 in. diameters and various ratios of length to diameter (b/a) dropped from rest through a copper tube. The average speed of fall is compared to predictions of the terminal velocity using Ref. 21 or Eq. (28). The last column is the predicted average velocity obtained by numerically integrating the equations of motion of a magnet experiencing the drag force given by Eq. (27).

No.	b/a	m (g)	μ (A m^2)	v_{average} (m/s)	v_t [a]	v_t [b]	V_{average}
1	1.0	12.1	1.76	0.0687	0.0669	0.0670	0.0674
2	1.5	17.9	2.36	0.1045	0.1050	0.1050	0.1058
3	2.0	23.8	3.23	0.1275	0.1243	0.1243	0.1254
4	3.0	36.4	5.00	0.1825	0.1710	0.1711	0.1731
5	4.0	48.2	6.37	0.2473	0.2451	0.2451	0.2486
6	1.0	12.9	1.17	0.1513	0.1615	0.1616	0.1622

[a]Reference 21.
[b]Equation (28).

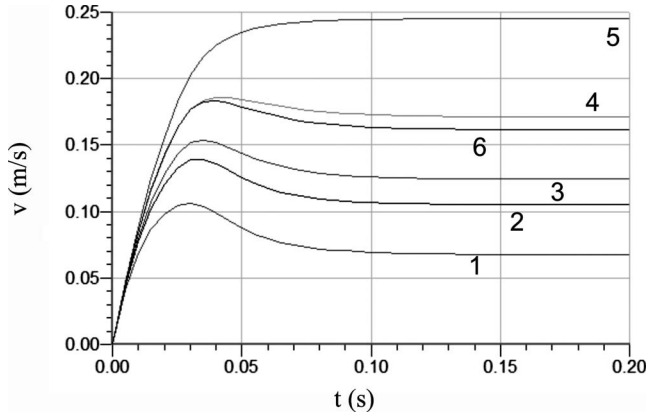

Fig. 3. Speeds of magnets dropped through a copper tube. Each magnet was inserted into the tube and then released from rest. The plots are numerical solutions of the equation of motion including the drag force during the first fifth of a second after release.

thus the total time of fall. Because of their differing lengths, the center of each magnet started out at a different height in the tube, resulting in slight differences in their initial behaviors. Figure 3 shows that the terminal velocity was achieved within a few tenths of a second, resulting in terminal speeds that are only slightly smaller than the average speeds of fall.

Even though the experimental procedures were not very sophisticated, there was excellent agreement between theory and experiment. The experiment thus seems to be within the capabilities of introductory students. How much of the simulations would be appropriate to ask them to do? That depends on the level of the class and the amount of time allotted to this project. It is possible to perform the computation of the terminal velocity at an introductory level if students are comfortable with spreadsheet programs. This simplification is possible for three reasons. First, the function C can be added to a spreadsheet as a user-defined function (see Appendix A), and B_ρ can be computed and graphed. Second, B_ρ is a symmetrical function of z, and thus the integral for v_{terminal} in Eq. (28) needs only to be evaluated from 0 to ∞. And third, at large enough values of z, B_ρ approaches the dipole form (Eq. (14)) and thus $B_\rho^2 \sim z^{-8}$ in the integrand for v_{terminal}, allowing the integral to be truncated at relatively small values of z. Students can plot B_ρ^2 in a spreadsheet and see that it starts at 0 at $z=0$, reaches a sharp maximum near $z=b$, and decreases by several orders of magnitude by $z=3b$. As a result, the entire integral may be computed as a simple Riemann sum from $z=0$ to about $z=3b$ using a step size $\Delta z \simeq 0.01b$. Any concern about truncation errors could be addressed by calculating the remainder of the integral analytically using the dipole approximation for B_ρ. More advanced students might be acquainted with other programs or numerical methods for handling these tasks, but the elementary method we have described gives results that are within about 1% of the results of the more sophisticated tools and can easily be improved by using smaller size steps.

V. COMMENTS

We have presented compact expressions for the magnetic field of an ideal solenoid and have demonstrated that they are easy to use, remarkably fast, and can readily be incorporated into spreadsheet calculations, making it possible to simulate a variety of situations involving cylindrical magnets. For the falling magnet demonstration, we have shown that a simple treatment provides results that agree with those from a more complicated analysis and are consistent with simple measurements. The methods used here can be applied to other cylindrically symmetric situations such as the electric fields of uniformly charged rings or cylindrical shells. Such fields can then be written in terms of the C function with all the advantages that have been described here.

We hope that these expressions for the magnetic field will help dispel the notion that exact expressions for the field of an ideal solenoid are necessarily complicated or computationally slow and will encourage student investigations of magnetic phenomena.

ACKNOWLEDGMENTS

The authors wish to acknowledge the support and assistance of John Belcher and the Center for Educational Computing Initiatives at the Massachusetts Institute of Technology.

APPENDIX A: GENERALIZED COMPLETE ELLIPTIC INTEGRAL

The generalized complete elliptic integral in Eq. (1) can be efficiently computed using an algorithm by Bulirsch[22] based on work of Bartky[23] who extended ideas of Landen and Gauss. This algorithm converges so quickly that unless $k_c \ll 1$, only three or four passes are necessary. The code shown in Fig. 4 is in a version of BASIC that can be loaded as a user-defined function to the CALC spreadsheet program (part of the *OpenOffice* (Ref. 24) software suite) where it can be used as a normal spreadsheet function, making C accessible to nonprogrammers. Similarly, *Microsoft Excel* allows user-defined functions coded in *Visual Basic*. This code is simple enough to be treated as pseudocode that can be easily adapted to other languages. Programs in FORTRAN and C code may be downloaded[25] or found in the first edition of *Numerical Recipes*.[26] Code in various programming languages is also available from the authors.

Later editions of *Numerical Recipes* no longer mention the C function and adopt Carlson's more general approach, which applies to incomplete as well as complete elliptic integrals. In terms of Carlson's functions, R_F and R_C, C is

$$C(k_c,p,c,s) = cR_F(0,k_c^2,1) + \tfrac{1}{3}(s-pc)R_J(0,k_c^2,1,p). \quad \text{(A1)}$$

Code for computing Carlson's functions may be found in the current editions of *Numerical Recipes*[27] and elsewhere. For complete elliptic integrals, Bulirsch's algorithm is more compact and also has some other advantages.[28] This generalized complete elliptic integral includes all three standard Legendre forms as special cases,

$$K(k) = C(k_c,1,1,1), \quad E(k) = C(k_c,1,1,k_c^2),$$

$$\Pi(n,k) = C(k_c,n+1,1,1), \quad \text{(A2)}$$

where $k=\sqrt{1-k_c^2}$. In algebraic work, the following identity is useful:

$$C(k_c,\gamma^2,2-\gamma,\gamma) - C(k_c,1,1,1) \equiv (1-\gamma)C(k_c,\gamma^2,1,\gamma). \quad \text{(A3)}$$

```
REM macro for Calc spreadsheet
FUNCTION cel(kc, p, c, s)
     IF (kc = 0) THEN
          cel = "NaN"
          EXIT FUNCTION
     ENDIF
     errtol = .000001
     k = ABS(kc)
     pp = p
     cc = c
     ss = s
     em = 1.
     IF (p > 0) THEN
          pp = SQR(p)
          ss = s/pp
     ELSE
          f = kc*kc
          q = 1. - f
          g = 1. - pp
          f = f - pp
          q = q*(ss - c*pp)
          pp = SQR( f/g )
          cc = (c - ss)/g
          ss =  - q/(g*g*pp) + cc*pp
     ENDIF
     f = cc
     cc = cc + ss/pp
     g = k/pp
     ss = 2*(ss + f*g)
     pp = g + pp
     g = em
     em = k + em
     kk = k
     WHILE (  abs( g - k ) > g*errtol  )
               k = 2*SQR(kk)
                kk = k*em
                f = cc
               cc = cc + ss/pp
               g = kk/pp
               ss = 2*(ss + f*g)
               pp = g + pp
               g = em
               em = k + em
     WEND
     cel = (pi/2.)*(ss + cc*em)/( em*(em + pp) )
END FUNCTION
```

Fig. 4. Algorithm for the generalized complete elliptic integral $C(k_c,p,c,s)$ coded in a version of BASIC for use as an add-in function in the CALC spreadsheet.

APPENDIX B: DERIVATION OF THE SOLENOID FIELD

The magnetic field of an ideal solenoid can be computed directly from the Biot–Savart law. The necessary algebra is only slightly more complicated than that which is needed to derive Eq. (2), which is commonly presented to students in introductory courses.

The surface of the solenoid is divided into circular strips of width dz' as in Fig. 5. The current in such a strip is $nIdz'$. To calculate the field at a point $\mathbf{x}$, we apply the Biot–Savart law to this circular loop and then sum the fields of the stack of strips that form the solenoid surface,

$$\mathbf{B}(\mathbf{x}) = \int_{-b}^{b} \frac{\mu_0}{4\pi} \oint (nIdz') \frac{d\mathbf{x}' \times \mathbf{R}}{|\mathbf{R}|^3}, \tag{B1}$$

where $\mathbf{R}=\mathbf{x}-\mathbf{x}'$, and points along the strip are specified by the position vector

$$\mathbf{x}' = a \cos \varphi' \hat{\mathbf{i}} + a \sin \varphi' \hat{\mathbf{j}} + z' \hat{\mathbf{k}}, \tag{B2}$$

and an infinitesimal step taken along the strip is

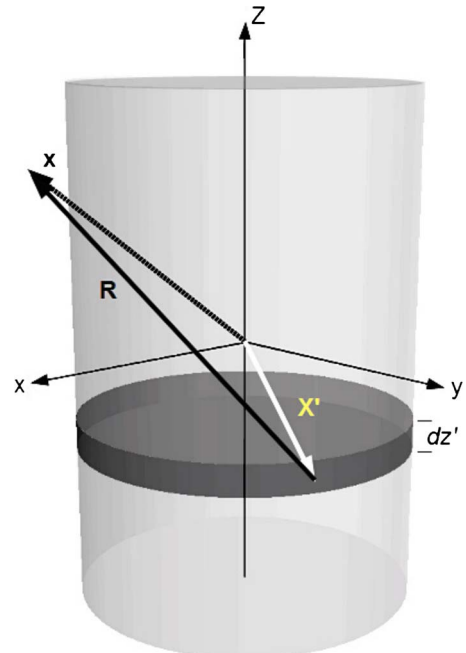

Fig. 5. Geometry of an ideal solenoid showing the notation used in applying the Biot–Savart law.

$$d\mathbf{x}' = (-a \sin \varphi' \hat{\mathbf{i}} + a \cos \varphi' \hat{\mathbf{j}}) d\varphi'. \tag{B3}$$

Because of cylindrical symmetry, we are free to choose coordinates in which $\mathbf{x}$ lies in the $x-z$ plane, causing $B_y(\mathbf{x})$ to vanish and allowing $B_x(\mathbf{x})$ to be identified with $B_\rho(\mathbf{x})$, prompting the notation

$$\mathbf{x} = \rho \hat{\mathbf{i}} + z \hat{\mathbf{k}}. \tag{B4}$$

Because

$$\mathbf{R} = (\rho - a \cos \varphi') \hat{\mathbf{i}} - a \sin \varphi' \hat{\mathbf{j}} + (z - z') \hat{\mathbf{k}}, \tag{B5}$$

and

$$d\mathbf{x}' \times \mathbf{R} = a d\varphi' [(z - z') \cos \varphi' \hat{\mathbf{i}} + (z - z') \sin \varphi' \hat{\mathbf{j}} + (a - \rho \cos \varphi') \hat{\mathbf{k}}], \tag{B6}$$

the field can be written as

$$\mathbf{B}(\mathbf{x}) = \int_{-b}^{b} dz' \left(\frac{\mu_0 nIa}{2\pi} \right) \int_0^{\pi} d\varphi' \times \frac{(z - z') \cos \varphi' \hat{\mathbf{i}} + (a - \rho \cos \varphi') \hat{\mathbf{k}}}{[\rho^2 - 2a\rho \cos \varphi' + a^2 + (z - z')^2]^{3/2}}. \tag{B7}$$

Integration over z' is elementary,

$$B_\rho(\mathbf{x}) = \left(\frac{-B_0 a}{2} \right) \int_0^{\pi} d\varphi' \cos \varphi' \times \left[\frac{1}{\sqrt{z_+^2 + \rho^2 + a^2 - 2a\rho \cos \varphi'}} - \frac{1}{\sqrt{z_-^2 + \rho^2 + a^2 - 2a\rho \cos \varphi'}} \right] \tag{B8}$$

and

$$B_z(\mathbf{x}) = \left(\frac{B_0 a}{2}\right)\int_0^{\pi} d\varphi' \frac{(a-\rho\cos\varphi')}{(\rho^2+a^2-2a\rho\cos\varphi')} \times\left[\frac{z_+}{\sqrt{z_+^2+\rho^2+a^2-2a\rho\cos\varphi'}} - \frac{z_-}{\sqrt{z_-^2+\rho^2+a^2-2a\rho\cos\varphi'}}\right]. \tag{B9}$$

To put these expressions into a form resembling the definition of the C function, we introduce a change in integration variable,

$$2\psi \equiv \pi - \varphi', \tag{B10}$$

and after using some trigonometric identities, we observe that

$$z_\pm^2+\rho^2+a^2-2a\rho\cos\varphi' = [z_\pm^2+(\rho+a)^2] \times(\cos^2\psi + k_\pm^2\sin^2\psi). \tag{B11}$$

The radial component of the field then becomes

$$B_\rho(\mathbf{x}) = B_0\int_0^{\pi/2} d\psi(\cos^2\psi-\sin^2\psi) \times\left[\frac{\alpha_+}{\sqrt{\cos^2\psi+k_+^2\sin^2\psi}} - \frac{\alpha_-}{\sqrt{\cos^2\psi+k_-^2\sin^2\psi}}\right]. \tag{B12}$$

Upon comparing each of the terms in this integrand to the integrand in the definition of C in Eq. (1), we recognize that the radial field can be identified as Eq. (3).

Similarly, the longitudinal component of the field becomes

$$B_z(\mathbf{x}) = \frac{B_0 a}{(\rho+a)}\int_0^{\pi/2} d\psi \frac{\cos^2\psi+\gamma\sin^2\psi}{\cos^2\psi+\gamma^2\sin^2\psi} \times\left[\frac{\beta_+}{\sqrt{\cos^2\psi+k_+^2\sin^2\psi}} - \frac{\beta_-}{\sqrt{\cos^2\psi+k_-^2\sin^2\psi}}\right], \tag{B13}$$

which can be recognized as Eq. (4).

To determine the magnetic field of a current loop ($0<b \ll a$), it is simplest to return to Eqs. (B8) and (B9), treat b as a small quantity, and expand the integrands to first order in b. Then repeat the transformations in Eqs. (B10) and (B11) to express the integrals in forms resembling the C function. The results are given in Eqs. (11) and (12).

[a]Electronic mail: nderby1@comcast.net
[b]Electronic mail: stanolbert@comcast.net

[1]John T. Conway, "Exact solutions for the magnetic fields of axisymmetric solenoids and current distributions," IEEE Trans. Magn. **37**(4), 2977–2988 (2001).
[2]Velimir Labinac, Natasa Erceg, and Dubravka Kotnik-Karuza, "Magnetic field of a cylindrical coil," Am. J. Phys. **74**(7), 621–627 (2006).
[3]Milan Wayne Garrett, "Axially symmetric systems for generating and measuring magnetic fields. Part I," J. Appl. Phys. **22**(9), 1091–1107 (1951).
[4]Edmund E. Callaghan and Stephen H. Maslen, "The magnetic field of a finite solenoid," NASA TN D-465 (1960), <ntrs.nasa.gov>.
[5]Andreas Sundquist, "Dynamic line integral convolution for visualizing streamline evolution," IEEE Trans. Vis. Comput. Graph. **9**(3), 273–282 (2003); available at <web.mit.edu/viz/soft/>.
[6]For source code see <web.mit.edu/viz/soft/>.
[7]E. B. Rosa and F. W. Grover, "Formulas and tables for the calculation of mutual and self induction," Bur. Stand. (U.S.), Bull. **8**(1), 53–77 (1911), <www.g3ynh.info/zdocs/refs/Rosa-Grover1911/Contents.html>.
[8]G. R. Olshausen, "Absolute formulae for the mutual inductance of coaxial solenoids," Phys. Rev. (Series I) **35**(2), 148–152 (1912).
[9]Milan Wayne Garrett, "Calculations of fields, forces and mutual inductances of current systems by elliptic integrals," J. Appl. Phys. **34**, 2567–2573 (1963).
[10]K. D. Hahn, E. M. Johnson, A. Brokken, and S. Baldwin, "Eddy current damping of a magnet moving through a pipe," Am. J. Phys. **66**(12), 1066–1076 (1998).
[11]D. Amrani and P. Paradis, "Faraday's law of induction gets free-falling magnet treatment," Phys. Educ. **40**(4), 313–314 (2005).
[12]Yan Levin, Fernando L. da Silveira, and Felipe B. Rizzato, "Electromagnetic braking: A simple quantitative model," Am. J. Phys. **74**(9), 815–817 (2006).
[13]Jhules A. M. Clack and Terrence P. Toepker, "Magnetic induction experiment," Phys. Teach. **28**(4), 236–238 (1990).
[14]Reed College, Physics 100, <academic.reed.edu/physics/courses/phys100/Lab Manuals/Electromagnetic Induction/faraday.pdf>.
[15]Video lesson, falling magnets, <www.wikidebrouillard.org/index.php/Aimant_qui_tombe_au_ralenti>.
[16]J. A. Pelesko, M. Cesky, and S. Huertas, "Lenz's law and dimensional analysis," Am. J. Phys. **73**(1), 37–39 (2005).
[17]M. K. Roy, Manoj K. Harbola, and H. C. Verma, "Demonstration of Lenz's law: Analysis of a magnet falling through a conducting tube," Am. J. Phys. **75**(8), 728–730 (2007).
[18]B. A. Knyazev, I. A. Kotel'nikov, A. A. Tyutin, and V. S. Cherkasskii, "Braking of a magnetic dipole moving with an arbitrary velocity through a conducting pipe," Phys. Usp. **49**, 937–946 (2006).
[19]J. Iñiguez, V. Raposo, A. Hernández-López, A. G. Flores, and M. Zazo, "Study of the conductivity of a metallic tube by analysing the damped fall of a magnet," Eur. J. Phys. **25**, 593–604 (2004).
[20]C. S. MacLatchy, P. Backman, and L. Bogan, "A quantitative magnetic braking experiment," Am. J. Phys. **61**(12), 1096–1101 (1993).
[21]M. Hossein Partovi and Eliza J. Morris, "Eddy current damping of a magnet moving through a pipe," Can. J. Phys. **84**, 253–274 (2006).
[22]Roland Bulirsch, "Numerical calculation of elliptic integrals and elliptic functions," Numer. Math. **7**, 78–90 (1965).
[23]W. Bartky, "Numerical calculation of a generalized elliptic integral," Rev. Mod. Phys. **10**, 264–269 (1938).
[24]The open source *OpenOffice* software suite is available at <www.openoffice.org>.
[25]FORTRAN code for evaluating the C function in Eq. (1) is available at <docdb.fnal.gov/ILC/sid/stanitz/ilcsoft-latest/cernlib-2006/src/mathlib/gen/c/religc64.F>.
[26]William H. Press, Brian Flannery, Saul A. Teukolsky, and William T. Vetterling, *Numerical Recipes in C* (Cambridge U. P., New York, 1988).
[27]William H. Press, Brian Flannery, Saul A. Teukolsky, and William T. Vetterling, *Numerical Recipes: The Art of Scientific Computing*, 3rd ed. (Cambridge U. P., New York, 2007).
[28]K.-D. Reinsch and W. Raab, "Elliptic integrals of the first and second kind: Comparison of Bulirsch's and Carlson's algorithms for numerical calculation," in *Special Functions, Proceedings of the International Workshop*, edited by Charles Dunkl, Mourad Ismail, and Roderick Wong (World Scientific, Singapore, 1999), pp. 293–308, <www-m2.ma.tum.de/homepages/kladire/publications/bucavgl/bucavgl.html>.